A Landslide Due to Long Term Creep

Un glissement dû au fluage de longue durée

by L. Šuklje, Dr. Techn., Professor, and S. Vidmar, Civ. Eng., Assistant, University of Ljubljana, Yugoslavia

Summary

The authors describe a landslide which occured along the Gradot ridge in Macedonia in 1956, when about 20 million cubic metres of silt and sand, covered by a volcanic deposit, slipped and filled the valley of the torrential Vatasha river to a depth of 70 metres.

This landslide lastened for only a few minutes, occuring along a plane of soft clay as the culmination of creep over a considerable period. Owing to unequal creep deformation of the underlying cohesive strata, the cohesion of the sandstone, of the conglomerate and of the volcanic overburden was overcome decades or even centuries before the landslide took place. Later the shear strength of the over-consolidated cohesive lower strata was overcome by creep which occured over a long period. Dynamic earthquake effects contributed towards craking of rigid strata and also helped to sustain the creep of the cohesive soil.

Immediately before this failure, only the friction corresponding to the actual pressure of the overburden and to the uplift caused by underground water, represented the shear strength of the slope. Using the effective stress method and assuming that $c' = 0$, an average factor of safety of 1·14 would appear to cover the effect of long term creep on the reduction of frictional resistance.

Sommaire

Environ 20 millions de m³ de sédiments lacustres néogènes formés de limon et de sable limoneux à la partie inférieure, de sable et de gravier plus ou moins liés à la partie supérieure, le tout recouvert par une dalle de tuf, se sont éboulés en 1956 de la crête de Gradot en Macédoine.

Les masses ont rempli la vallée de la rivière Vatacha sur 70 m de hauteur. Le glissement qui s'est produit en quelques minutes le long d'une base argileuse peu inclinée, représente la phase finale d'un fluage de longue durée. En raison des déformations de fluage non uniformes des couches cohérentes sous-jacentes, la cohésion des grès, des conglomérats et des tufs a été éliminée des dizaines ou des centaines d'années avant le glissement. Après quoi, la résistance au cisaillement des couches cohérentes préconsolidées a été épuisée progressivement pendant une longue période de fluage. Les effets dynamiques des secousses sismiques ont contribué à la fissuration initiale des couches rigides ainsi qu'à l'entretien du fluage des sols cohérents.

Immédiatement avant la rupture, seul le frottement correspondant à la surcharge réelle compte tenu de la poussée de l'eau contribuait à la résistance du talus. En employant la méthode des contraintes effectives et en supposant $c' = 0$, l'effet du fluage de longue durée sur la diminution de la résistance au frottement, peut être exprimé par un coefficient de sécurité apparente $F = 1{,}14$.

Failure

On the morning of September 5th 1956 the west slope of the Gradot ridge in Macedonia slid along a length of 800 m and filled the valley of the Vatasha river up to a height of 70 m (Fig. 2). Two groups of people were caught by the slide on the road running along the slope (Fig. 4), and two farmers in the field below the road. The farmers and the northern group of twelve people began to run when stones started falling from overhead and the soil moved under their feet. They reached firm ground just in time. Only the man who went back to save his horse, was swallowed up by the sliding earth. Two or three minutes after the first indications of movement the slope collapsed with a thunderous roar and a huge cloud of dust appeared above the valley. A second group of five people was delayed by the filling up of the crack which appeared on the southern boundary of the landslide, for their horse and carriage could not pass. As they proceeded they were alarmed by the collapse of the northern part of the slope, approximately up to the profile c - c shown on Fig. 4. A few minutes later the entire southern part of the slope, on which they were standing, began to slide. They were moved with the sliding mass for a distance of about 130 metres. The earth was cracking under their feet, but three men saved themselves, a woman and a child by a desperate leap. After the failure, the earth rocked for about twenty minutes before coming to a standstill; local displacements continued until the following day.

Eleven shepherds and several flocks of sheep were buried in the valley under the landslide which left behind 130 metre high wall of the broken mountain.

Preceding cracks

Along the upper boundary of the slide a discontinuous series of deep cracks were formed between elevations 664 and 716 (Fig. 4) over a length of about 270 m. The oldest people had known these since their childhood and thirty years ago a man descended by means of a rope to a depth of 30 m but did not reach the bottom. The cracks were separated in the upper part only by loosened and fractured material, but their depth was continuous. The longest was about 20 m long and 130 cm wide. A year before the failure the lower boundary of the cracks was observed to have subsided for 20 cm. Further subsidence appeared some weeks before the failure, and natural bridges, separating single cracks, broke off. In the morning stillness, noises were heard from the depth of the cracks. At the same time, a step appeared on the road along the southern boundary of the slide.

Geological data

The Gradot ridge is situated 22°5′ *E* from Greenwich on 41°15′ north latitude, 8 to 10 km *SSE* from the small town Kavadarci. It belongs to a tableland formed by erosion action. The ridge stretches between the Vatasha river and its affluent the Sadjavica (Fig. 4).

Fig. 1 Landslide panorama. (The rubble slope on the toe of the break-off wall proceeds from blowing up the cap of the hill after failure.)
Vue panoramique du glissement. (Les débris au pied de la crête rompue proviennent du sautage du sommet après le glissement.)

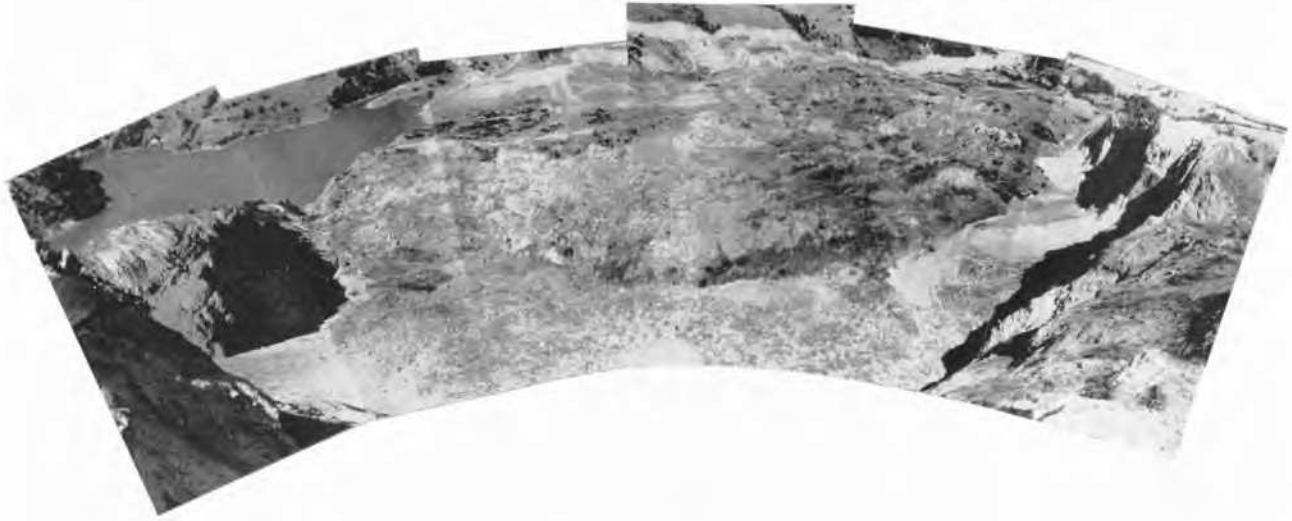

Fig. 2 View from the top of the ridge. On the left is the lake created by the landslide acting as a dam. In the middle background are the provisional spillways, the final spillway under construction and the erosion bed from 1957, and on the right the valley of the Vatasha river downstream from the landslide.

Vue prise du sommet de la crête. A gauche, on peut voir le lac qui a été créé par le remblai provenant du glissement ; dans la partie centrale, le déversoir provisoire, le déversoir définitif en construction et le lit creusé par la crue en 1957 ; à droite, la vallée de la rivière Vatacha en aval du glissement.

Fig. 3 The erosion bed created by the overflow of floodwater in 1957.

Le lit creusé par la crue en 1957.

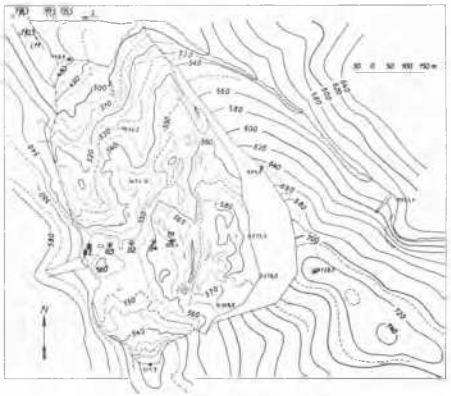

Fig. 5 Plan of the landslide after failure. The full line passing through elevation 664, represents the original break-off boundary of the landslide, and the thin dotted line passing through elevation 728·5, represents the present boudanry formed after blowing up the top of the ridge. Small circles with tails illustrate the actual springs. *LM* = Vatasha river (called also Luda Mara), *S* = Sadjavica torrent.

Vue en plan du glissement après la rupture. La ligne pleine passant par la cote 664 représente la limite supérieure initiale du glissement, tandis que la ligne fine interrompue représente la limite actuelle formée après le sautage. Les petits cercles à queues représentent les sources actuelles. *LM* = la rivière Vatacha (appelée aussi Luda Mara), *S* = l'affluant Sadjavica.

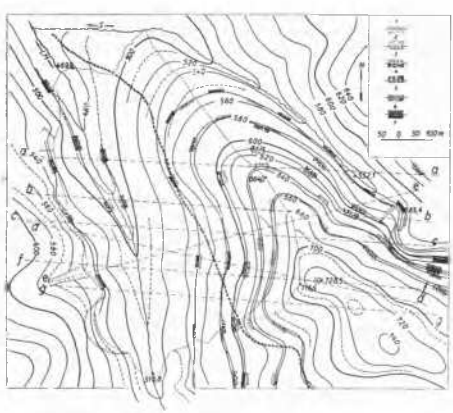

Fig. 4 Plan of the territory before the failure. The landslide boundary is marked by a thin full line passing through the elevations 716·6, 664·0, 469·9 and 516·8. Geological boundaries are marked by thick full lines rimmed by layer markings with the following designation : 1 = andesite tuff, 2 = sand and gravel well bound, 3 = conglomerate, 4 = sand and gravel weakly bound, 5 = gravel not strongly bound, 6 = silt with silty sand intercalations, 7 = clay. *b-b* and *d-d* = the directions of geological profiles presented in Fig. 6 ; *a-a*, *b-b*, *e-e*, *f-f* and *g-g* = the directions of cross sections analysed (Fig. 12 and table 2).

Vue en plan de l'aire de glissement avant la rupture. La limite du glissement est marquée par une mince ligne pleine passant par les cotes 716·6, 664·0, 469·9 et 516·8. Les limites géologiques sont marquées par des lignes épaisses pleines bordées des marques des couches dont la signification est la suivante : 1 = tuf andésitique, 2 = sable et gravier bien liés, 3 = conglomérat, 4 = sable et gravier faiblement liés, 5 = gravier faiblement lié, 6 = limon et sable limoneux, 7 = argile. *b-b* et *d-d* = directions des coupes géologiques présentées sur la Fig. 6 ; *a-a*, *b-b*, *e-e*, *f-f* et *g-g* = les directions des coupes soumises à l'analyse de la rupture (Fig. 12 et le tableau 2).

North of the profile *c-c* (Fig. 4) the Vatasha river has cut into the clayey lacustrine sediments belonging to Pliocene deposits. The strata contain rare and shallow sandy intercalations and are falling at a constant slope in the north westerly direction at a dip of about 4°. On the plan (Fig. 4) and on the geological cross-sections (Fig. 6), the clay series is marked by the number 7.

Above the clay stratum, layers of silt alternate with sandy silt deposits. The whole series (Fig. 6) is 45 m thick and belongs to the same geological formation as its base.

The plastic silty and clayey sediments are covered by a big slab consisting of two horizons. The lower horizon (layers 5 to 2 inclusive in Figs. 4 and 6) is about 100 m thick and consists of sandy and gravelly sediments with some silty intercalations and admixtures. Sands and gravels consist mainly of andesite and contain tuff lapilli. They pass on to sandstones and conglomerates which are partly loose and partly firm. The detailed stratification is shown in Fig. 6. The andesitic tuffs of the upper horizon appear in breccia and sandstone form as a rigid stratum up to 70 m thick. The eruptions lasted still in Pleistocene period.

All the above strata are approximately parallel to the clay base (NW 78° under 4°).

The chenozoik sediments, the whole thickness of which is about 3 000 m, lie unconformably above the folded and tectonically damaged older ground. The Gradot ridge is situated at the crossing point of the dinaric (NW-SE) and the transversal tectonic direction (NE-SW). The earthquakes, the epicentres of which commonly appear in such tectonic lines, have been very numerous in recent years. As stated by

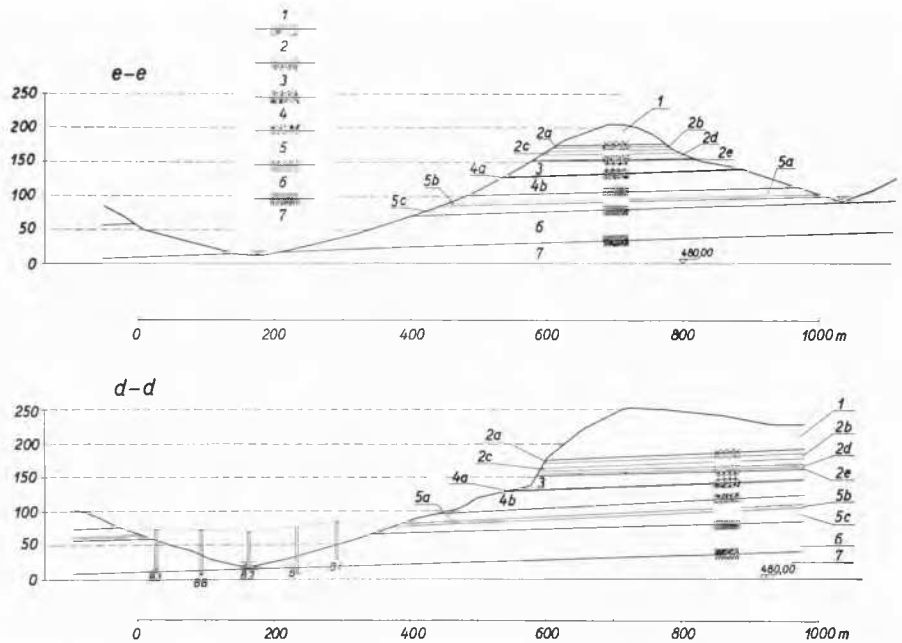

Fig. 6 Geological cross sections *b-b* and *d-d* (see Fig. 3). The explanation of layer markings 1 to 7 given in the legend to figure 3, may be completed by the following specifications : 2 *a* = gravel and sand inadequatly bound (thickness $h = 2$ m); 2 *b* = andesite lapilli (diameter up to 50 cm) consolidated by fine gravel and sand ($h = 9$ m) ; 2 *c* and 2 *d* = well bound sandy gravel ($h = 14$ m) ; 2 *e* = silt (0·9) m ; 4 *a* = a thin layer of decomposed tuff ; 4 *b* = sand and fine gravel with lapilli up to 30 cm in diameter ($h = 30$ m) ; 5 *a* = 5 *c* = strongly bound conglomerate ($h = 41$ m) ; 5 *b* = silty sand ($h = 4$ m).

Coupes géologiques *b-b* et *d-d* (voir Fig. 3). L'explication des signes des couches qui a été donnée dans la légende à la figure 3, doit être complétée par les spécifications suivantes : 2 *a* = gravier et sable faiblement liés (épaisseur $h = 2$ m) ; 2 *b* = lapilli d'andésite (jusqu'à 50 cm de diamètre) liés avec du gravier fin et du sable ($h = 9$ m) ; 2 *c* et 2 *d* = gravier sableux bien lié ($h = 14$ m) ; 2 *e* = limon (0·9 m) ; 4 *a* = une couche mince du tuf andésitique décomposé ; 4 *b* = sable et gravier avec lapilli jusqu'à 30 cm de diamètre ($h = 30$ m) ; 5 *a* = 5 *c* = conglomérat bien lié ($h = 41$ m) ; 5 *b* = sable limoneux ($h = 4$ m).

Mihajlović (1956) 1628 earth-quakes have been noticed in the area of the Vardar river during the period from 1906 to 1942, and some of them exceeded the intensity IX of the MOS scale. The epicentre of the earthquake of March 8th 1931 with an intensity from IX to X was about 40 km distant from Gradot.

Hydrological data

Many springs were in evidence on the right bank downstream from the cross-section *c-c* (Fig. 4) some metres above the river bed. They appeared just on the upper boundary of the clayey series (7) and did not dry even during intense drought.

After the landslide the water flowed out of the broken mountain down from the sandy silty layers 2e, 4a and 5b (Fig. 6). Considering the limited area of rainfall above these layers and the small annual precipitation (600 mm on an average), it is hardly likely that the underground waters above the less pervious silty intercalations formed a continuous potential reservoir. Since no springs appeared on the slope crossing lines of the above mentioned silty layers, it can be assumed that the water flowed through the loosened material and the cracks on the slip plane towards the impervious clayey base, and the sandy layers in the sandy silt series (6) watered the springs.

The Vatasha river is of torrential type. It swells in spring and in autumn. The maximum flow under flood conditions is estimated to be as high as 150 cub. m. per sec., but commonly it does not exceed 30 cub. m per sec. Under summer drought conditions the river bed is dry and this was the case at the time when the landslide occured; the drought was preceded by extremely sultry weather. In 1957, before satisfactory spillways had been constructed, the floodwater overflowed the dam crest and some 600·000 cub. m of material has been eroded and swept away. The erosion bed is shown in Fig. 3.

Geotechnical properties of the landslide material

The plasticity characteristics of some samples of the clayey (7) and siltey (6) layers are presented in Fig. 7 and the corresponding grain-size curves in Fig. 8. The samples are designated by the number of the series (7 or 6) and by the depth (in metres) under the contact with the upper series (if meas-

ured). It can be seen that the plasticity of the clay layers near the contact is higher than at greater depth. Some activity values are given in table 1.

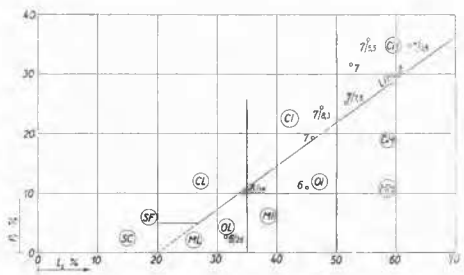

Fig. 7 *AC*-diagram. The samples are marked by layer number after the legends given in Figs 4 and 6. The second Arabic numeral represents the depth below the contact with the upper series.

Diagramme *AC*. Les échantillons sont marqués par les chiffres des couches selon les légendes données sur les figures 4 et 6. Les seconds chiffres arabes représentent la profondeur au dessous du contact avec la série supérieure.

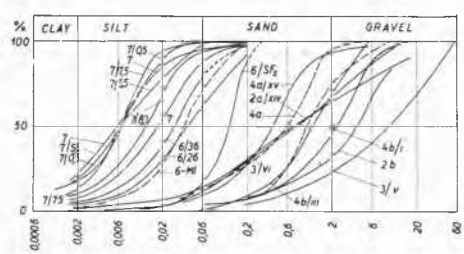

Fig. 8 Grain-size curves of some typical samples (marked as on Fig. 7). The boulders ($D > 60$ mm) have been sorted out before the mechanical analysis.

Courbes granulométriques de quelques échantillons typiques (marqués comme sur la Fig. 7). Les cailloux ($D > 60$ mm) ont été éliminés avant l'analyse granulométrique.

The shear strength of some characteristic remoulded samples has been tested in the triaxial as well as in the direct ring shear equipments. The results are presented in Fig. 9. A clay sample taken near the contact (7/0·5) and a silty sample (6-M1) have been subjected to long term ring shear apparatus tests. The results are presented in Figs 10 and 11. The rate of creep of the laboratory samples decreases approximately in inverse proportion to time up to 90 per cent of the shear strength. Comparing the measured shear strength values with those determined by usual Q_c tests and expressed in terms of effective stress (Figs 9 and 10) it can be seen that the preceding creep has no influence on the end value of shearing strength in laboratory test conditions. After the landslide the angle of shear resistance fell from 27° to 18° in the silty sample and from 24°20′ to 15°30′ in the clay sample. It is probable that the effect of long duration creep in geological conditions, sustained by negative thixotropic effects of earthquakes, can also reduce the shear strength.

The dissipation of shear strength shown on Fig. 9 has probably to be attributed partially to the sensitivity effects on the remoulded samples and partially to the volumetric change of the incompletely saturated triaxial samples in the Q_c tests. Taking into account such effects and disregarding the influence of preconsolidation, the following average values for shear angles φ' can be assumed for stability analysis :

clay (series 7) : 22°;

silt : 26°
sand : 31° } average value for the series 6 : 28°;

The grain size curves of some samples of the sandy and gravel series (5 to 2) are presented in Fig. 8 and the corresponding bulk densities are given in table 1 which also contains some permeability test results.

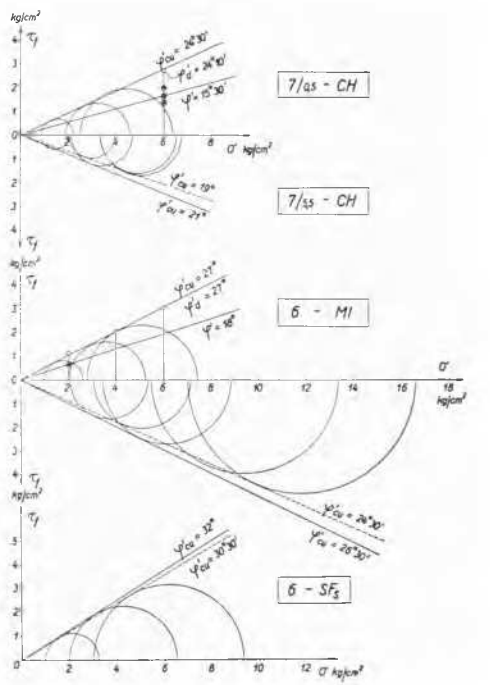

Fig. 9 Triaxial and ring shear test results. The shear strength values obtained by slow direct shearing tests are marked with single small circles and the corresponding values obtained by repeated shear, after the first shear, by small double circles.

Résultats des essais triaxiaux. Les valeurs de la résistance au cisaillement obtenus par des essais lents, exécutés dans les appareils de cisaillement par rotation, sont marquées par des petits cercles, et les valeurs correspondantes obtenues après la rupture primaire par cisaillement répété, sont marquées par des doubles petits cercles.

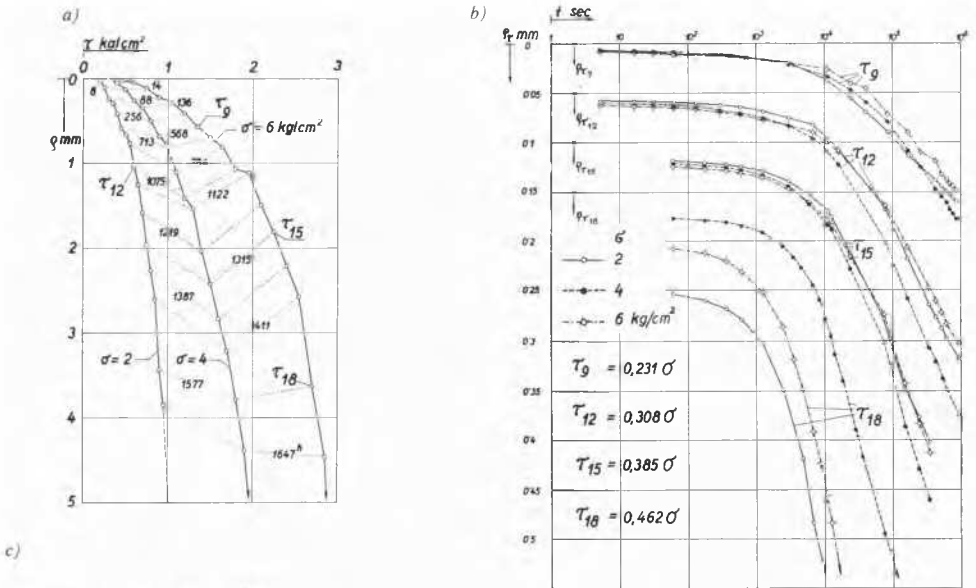

Fig. 10 Long term creep test of the silty sample 6-*M1*. (a) Shear stress τ versus shear displacement ρ curves with the notation (in hours) of the single load steps duration. (b) Shear displacement (ρ) versus logarithm of time (t) curves for load steps $n = 9$, 12, 15 and 18, $n = 40\ \tau/\sigma$. (c) Creep rate versus logarithm of time curves for the last load steps.

Essai de fluage de l'échantillon 6-*M1*. (a) Déplacement de cisaillement ρ en fonction de la contrainte de cisaillement τ avec indication (en heures) de la durée des degrés de chargement. (b) Déplacement de cisaillement ρ en fonction du logarithme du temps, pour les degrés de chargement $n = 9$, 12, 15 et 18, avec $n = 40\ \tau/\sigma$. (c) Vitesse du fluage en fonction du logarithme du temps pour les derniers degrés de chargement.

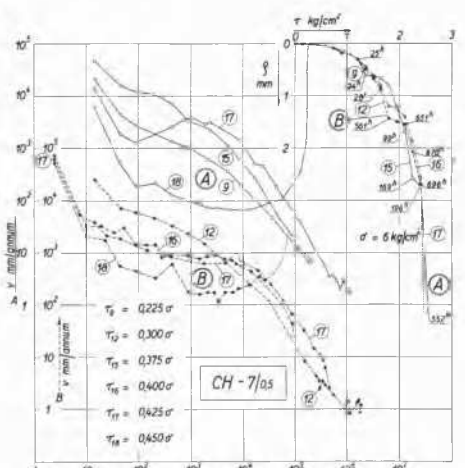

Fig. 11 Long term creep test of the clayey sample *CH*-7/0-5.
Essai de fluage de longue durée pour l'échantillon argileux *CH*-7/0-5.

Table 1

Layer/sample	*AC-classification*	*Activity*	*Sensitivity*	*Bulk density* γ t/m³	*Coefficient of permeability* k_{10} *at the consolidation pressure* p_0	
					k_{10} (cm/sec)	p_0 (kg/cm²)
7/0·5	CH	1·74	1·6	—	$1{\cdot}4 \cdot 10^{-8}$	2·0
7/5·5	CH	1·80	—	—	—	—
6/26	ML	0·65	—	—	—	—
6/30	ML-CL	1·8	—	—	—	—
6/M1	M1	5·5	1·6	(γ_s = 2·75)	$3{\cdot}9 \cdot 10^{-7}$	6·0
6/SF_s	SF_s	—	—	(γ_s = 2·71)	$6{\cdot}8 \cdot 10^{-6}$	6·0
4 b	SF_s	—	—	1·77	$6{\cdot}4 \cdot 10^{-6}$	4·0
4 a	SF_s	—	—	1·92	$2{\cdot}1 \cdot 10^{-6}$	4·0
3/binder	SP	—	—	1·72	—	—
3/tuff lapilli	—	—	—	2·36	—	—
2 d	G	—	—	1·82	—	—
2 a	G	—	—	1·96	—	—
1	tuff	—	—	2·12	—	—

Table 2

Cross section (see Figs 3 and 12)	*Slip surface in the clayey series* r = *radius* (m) d = *the greatest depth below the contact* (m)	*Activated shear angles* φ' *in the layer series*			*Apparent safety factor* F				
		2-5 *(sand and gravel)*	6 *(silt and silty sand)*	7 *(clay)*	*Single values in the layer series* 2-5	6	7	*Average values for the most unfavorable slip surfaces*	
a-a	Along the upper contact	32° 40′	22° 30′	18° 15′	1·22			→	1·14
		38°	28°	15°	1	1	1·50	1·18	
b-b		34° 10′	24° 50′	19° 30′	1·14			→	
		38°	28°	17° 40′	1	1	1·26		
f-f		36° 55′	27° 5′	21° 15′	1·04			→	
		38°	28°	20° 30′	1	1	1·08	1·09	
	r = 572 d = 37			20° 20′			1·09		
	r = 378 d = 62			20° 20′			1·09		
				18°			1·24		
	r = 330 d = 92	33° 20′	24° 10′	18° 40′	1·19				
g-g	Along the upper contact	34° 25′	25°	19° 45′	1·14			→	
		38°	28°	17°	1	1	1·32		
e-e		33° 30′	24° 15′	18° 45′	1·19				
		38°	28°	16°	1	1	1·40		

Failure analysis

The shear strength values at failure have been investigated by the Swedish graphical slices method. Allowance was made for the fact that the rigid cap of tuff did not participate in the shear strength, for it was dislocated by the vertical crack. The slip plane of the series of sands and gravels (2 to 5) was laid bare by failure and its curved form could be found from land surveying data. As the material from the clayey series was not found in the bore holes *B*3, *B*4 and *B*1 * (Figs 5 and 6), it is certain that the slide occured on the upper boundary of this series. The stability analysis proved that the prolongation of the upper, circular part of the slip plane through the sandy silty series (6) represents the most unfavorable junction of the two above mentioned parts. The discontinuous slip plane obtained in this way agrees with the configuration of the slope and of the valley before and after the failure, as well as with the kinematics of the sliding.

The uplift forces have been taken into account corresponding to the probable saturation of the sandy and silty layers in the series 6, while the discontinuity of the upper underground water reservoirs was assumed. The cohesive part of the shearing strength was disregarded in all strata and the average shear angle of sand gravel has been assumed as high as 38°. Considering further the average shear angles of 28° for the sand silty series and 22° for the clayey base, the corresponding factor of safety was found by the usual method. The procedure is shown in Fig. 12 and the results in the same illustration, as well as in table 2. This table also contains the results corresponding to the assumption that full shear angle operated in sands and gravels (38°) as well as in the sandy silty series (28°).

Neglecting the effect of over-consolidation and considering the uplift also within the clay series, comparative values are given for some deeper, circular slip surfaces in the cross-section *f-f*. It can be seen that the corresponding apparent safety factors are greater than for the plane slip surface along the contact, although there is no appreciable difference between the factors of safety corresponding to the surfaces extending down to a depth of about 65 m below the contact. As the contact with the more permeable upper layers also represents the surface where the effect of over-consolidation can be more rapidly overcome, it is easy to understand why the sliding occurred just along the contact. Nevertheless, older and similar landslides on the left slopes of the Vatasha river downstream from Gradot which occured in the clayey layers with the inclination inside and towards the slope, show that the effect of over-consolidation can be eliminated within the clayey series.

The steep background slip surface with the circular cross section is also slightly curved in the horizontal direction. The fact that the northern part of the slope slipped first, although the apparent factor of safety is somewhat greater for the northern profiles a and *b* than for the southern profiles *f* and *g* (see Figs 4 and 12 as well as table 2), is probably due partly to the lateral friction effect and partly to the likely greater inflow of underground water towards the downstream part of the valley.

Hypothesis about failure conditions

The basic disposition for the landslide resulted from the erosive action of the river deepening its bed through the silty layers into the underlying clay series. The loading by a rigid slab 170 m thick of andesite sediments caused creep in the underlying layers of silt and silty sand as well as in their clay base. Due to the unequal creep deformations of

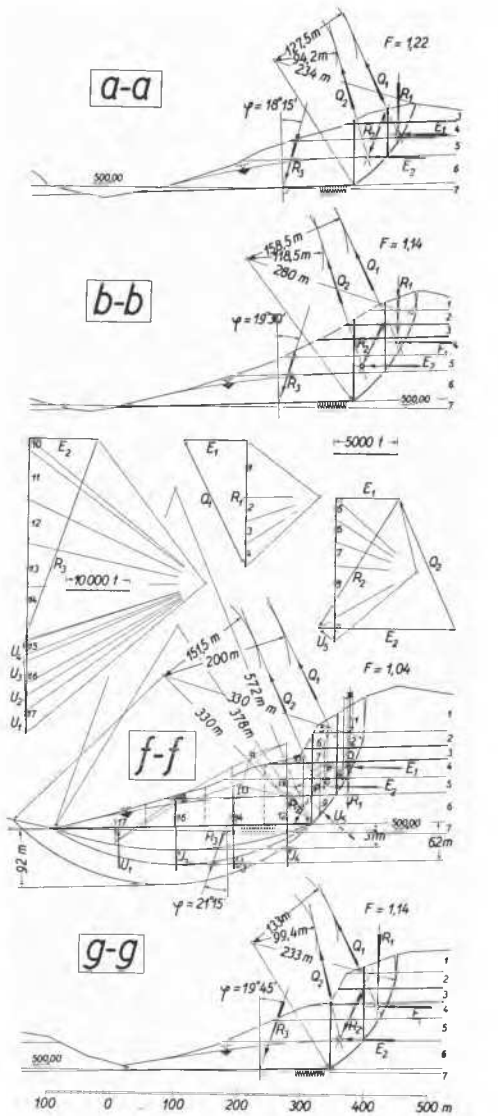

Fig. 12 Failure analysis results for the cross sections *a-a*, *b-b*, *f-f* and *g-g* (see Fig. 4). The complete procedure is shown only in the cross section *f-f* for the slip surface along the upper boundary of the clay series (7).

Résultats de l'analyse de rupture pour les coupes *a-a*, *b-b*, *f-f* et *g-g* (voir Fig. 4). L'analyse complète n'est présentée que dans la coupe *f-f* pour la surface de glissement suivant la limite supérieure de la série argileuse (7).

* These bore holes had been made in 1957 for the dam design purposes before our field investigation began.

the cohesive ground, an unfavourable state of stress occured in the conglomerates and in the cap of tuff. The dynamic effects of earthquakes contributed to failure. In this way the cohesive part of the more or less bound sands and gravels had been overcome in the most unfavourable shear direction, while a continuous vertical tension crack appeared in the rigid tuff cap. The cohesion of the over-consolidated * silty layers (6) and the adhesion at their contact with the clay were eliminated by progressive creeping which had been sustained by dynamic earthquake effects destroying the thixotropic effects of consolidation.

The width of the crack in the rigid tuff cap before sliding enables an estimate of creep displacement to be made after cracking and before the landslide. The average rate of creep in the last hundred years must have been smaller than 15 mm per year, but it increased progressively before the failure. Sliding probably occurred in a thin plastic zone and the failure can be interpreted as a line failure. The probable creep rates preceding the sliding are of the same order of magnitude as those found in the long term shear tests.

Conclusions

The landslide investigation and failure analysis give rise to the following conclusions :

(a) In slopes with heterogeneous stratification, the creeping of plastic underlying soil provokes unfavourable stress in the rigid overburden layers, causing shear or tension cracks to develop. In this way the shear strength of the upper layers is reduced to the friction part only or is even completely eliminated if the cracks are vertical.

(b) In the geological conditions of the Gradot landslide, the long term creep effects eliminated completely the cohesive part of the shear strength along the upper boundary of the clay layers as well as across the silty series, and reduced the friction part corresponding to the actual overburden pressure for about 15 per cent in comparison with the values, obtained by laboratory tests of the remoulded samples.

(c) The seismic effects tend to maintain creep both as a result of increased stress and negative thixotropic action.

* The pre-consolidation pressure surpassed the present overburden pressure in the plane clayey part of the slipe surface probably for about 120 to 500 tons per sq. m and in the curved silty part for 100 tons per sq. m on an average.

Acknowledgements

Field investigations and laboratory testing, the results of which are reviewed in this paper, were carried out in 1959 and 1960 by a research group of the Soil Mechanics Laboratory at the University of Ljubljana with the financial aid of the "Boris Kidrič" Fund. The authors are especially indebted to their colleagues Mr. F. Drobne, Geologist, for his important contribution regarding the geological mapring of the slide area, and Mr. V. Vazzas, Assistant, who was in charge of land surveying. Mr. R. Stojanov, Geol. Eng., Geological Institute of Macedonia, was kind enough to put the report of his previous geological investigations at the disposal of the authors.

Reference

[1] Mihajlović, J. (1956). Seizmološka karakteristika na terenot na jugozapadna i južna Makedonija. (The seizmic characteristic of the South West and South Macedonia. In Macedonian.) Trudovi na Geol. zavod na NRM, sv. 5, Skopje.